SHORT COMMUNICATION



Check for updates

Can we still measure circular dichroism with circular dichroism spectrometers: The dangers of anisotropic artifacts

Thomas J. Ugras^{1,2} | Yuan Yao³ | Richard D. Robinson^{2,3} |

¹School of Applied and Engineering Physics, Cornell University, Ithaca, New York, USA

²Kavli Institute at Cornell for Nanoscale Science, Ithaca, New York, USA

³Department of Materials Science and Engineering, Cornell University, Ithaca, New York, USA

Correspondence

Richard Robinson, Department of Materials Science and Engineering, Cornell University, Ithaca, NY 14853, USA.

Email: rdr82@cornell.edu

Funding information

Kavli Institute at Cornell, Cornell University; National Science Foundation, Grant/Award Numbers: CHE-2003586, DMR-2003431; Cornell Center for Materials Research, Grant/Award Number: DMR-1719875

Abstract

Chiral materials with strong linear anisotropies are difficult to accurately characterize with circular dichroism (CD) because of artifactual contributions to their spectra from linear dichroism (LD) and birefringence (LB). Historically, researchers have used a second-order Taylor series expansion on the Mueller matrix to model the LDLB interaction effects on the spectra in conventional materials, but this approach may no longer be sufficient to account for the artifactual CD signals in emergent materials. In this work, we present an expression to model the measured CD using a third-order expansion, which introduces "pairwise interference" terms that, unlike the LDLB terms, cannot be averaged out of the signal. We find that the third-order pairwise interference terms can make noticeable contributions to the simulated CD spectra. Using numerical simulations of the measured CD across a broad range of linear and chiral anisotropy parameters, the LDLB interactions are most prominent in samples that have strong linear anisotropies (LD, LB) but negligible chiral anisotropies, where the measured CD strays from the chirality-induced CD by factors greater than 10^3 . Additionally, the pairwise interactions are most significant in systems with moderate-to-strong chiral and linear anisotropies, where the measured CD is inflated twofold, a figure that grows as linear anisotropies approach their maximum. In summary, media with moderateto-strong linear anisotropy are in great danger of having their CD altered by these effects in subtle manners. This work highlights the significance of considering distortions in CD measurements through higher-order pairwise interference effects in highly anisotropic nanomaterials.

KEYWORDS

anisotropic samples, circular dichroism, differential Stokes–Mueller formalism, films, LDLB, linear dichroism, polarization modulation spectroscopy, true CD

1 | INTRODUCTION

The determination of optical activity and the measurement of circular dichroism (CD) in highly anisotropic samples presents an experimental challenge. 1-11 CD measurements were originally used to study samples in the solution state that were isotropic, meaning they had random, homogeneous arrangements of chromophores. Samples that contain optically active absorbing molecules organized with a preferred spatial orientation, however, cannot be accurately characterized by a typical CD measurement because of the influence of artifacts introduced by the anisotropy. The optical properties of oriented systems have been studied since the 1960s. 1,12-21 As the field has progressed to include more highly aligned solid-state samples and structured liquid crystal-like solutions, the assumption that samples are isotropic has been challenged. 9,22-27 This issue is becoming more significant with the emergence of highly oriented nanomaterials and metamaterials. Studies of interference between macroscopic anisotropies have grown in recent years and have even been proposed as a route to realize chiral polaritons for quantum transduction and information schemes. 2-7,9,28-33

The observed CD signal, or "measured CD," from a typical CD spectrometer can be modeled using the Stokes-Mueller formalism. As derived by the secondorder Taylor series expansion in the differential Stokes-Mueller formalism, the measured CD signal contains contributions from not only the intrinsic, chiralityinduced CD but also from linear dichroic (LD) and linear birefringent (LB) interaction terms (the "LDLB" terms). By flipping the sample along the light axis and averaging the resulting CD spectra, it is possible to eliminate the LDLB interference terms. This phenomenon was observed by Shindo et al.² and has recently been rigorously derived by our group⁷ to address linear contributions from our multiscale hierarchical nanomaterial structures.³⁴ (We note that flipping the sample does not eliminate the LDLB interference terms in the recently proposed case of helically stacked lamellae LDLB effects.⁵ In this case of helically stacked transition dipoles, the LDLB effects do not invert upon sample flipping because the chiroptic response is independent of sample orientation.⁵) For the most part, modeling the measured CD using expansions to the second-order is sufficient. 1,35 But as the chiral nanomaterials community engineers materials with strong linear anisotropy and g-factors approaching the theoretical limit, this second-order expansion is insufficient and may be relaying inaccurate approximations of the true, underlying contributions to the signal. 23-27,36-40 In this work, we derive expressions for the measured CD (I_{CD}) using the differential StokesMueller formalism with first-, second-, and third-order Taylor series expansions and consider the differences in the resultant expressions. After reinforcing the presence of second-order LDLB artifacts in linearly anisotropic samples, we find that the third-order expansion introduces terms that can make noticeable contributions to the simulated CD spectra in strongly linearly and circularly dichroic media.

2 | DERIVATION

In this section, we expand the derivation of the approximation to the measured CD (I_{CD}) to include higher-order terms. In our previous work, we derived expressions for the I_{CD} through differential Stokes–Mueller formalism with a second-order expansion. Here, we review the key steps of the previous derivation and extend it to present several new expressions for the measured CD.

Incident light propagating in the z-direction is described by the Stokes vector $(S)^{41}$:

$$S = \begin{bmatrix} I \\ Q \\ U \\ V \end{bmatrix} = \begin{bmatrix} I = I_x + I_y \\ I_x - I_y \\ I_{45^{\circ}} - I_{-45^{\circ}} \\ I_R - I_L \end{bmatrix}$$
(1)

where I is the total intensity of the light, Q is the difference in intensities between the x- and y-polarized light (I_x,I_y) , U is the difference in intensities between the $\pm 45^\circ$ polarized light $(I_{45^\circ},I_{-45^\circ})$, and V is the difference in intensities between the right- and left-circularly polarized light (I_R,I_L) . Throughout this work, we consider the Stokes vector to be normalized by holding the constraint $I^2 \geq Q^2 + U^2 + V^2$.

The Mueller matrix (M_z) is a matrix that describes an optical system with experimentally measurable quantities and connects the intensities and values of the input and output Stokes vectors $(S_{in}, S_{out}, \text{ respectively})$ to describe the light–matter interactions ^{43,44}:

$$S_{out} = M_z S_{in} \tag{2}$$

The Mueller matrix of a sample can be treated with the lamellar approximation, where the entire sample is broken down into infinitesimally thin slabs, the differential Mueller matrix (m), that are related to the Mueller matrix as a spatial derivative.^{7,31,44} For a non-depolarizing, uniform sample, the two matrix representations are related by $M_z = e^{mz}$ where:⁵

In these matrices and expressions, A represents the absorption, LD and LB represent the linear dichroism and linear birefringence, respectively, associated with the x- and y-axes, LD' and LB' represent their counterparts measured at $\pm 45^{\circ}$ relative to the original coordinate system, CD and CB represent circular dichroism and circular birefringence, respectively, 1 is the 4×4 identity matrix, and the lowercase notations are expressions in per unit length notation ($ld \equiv \frac{LD}{z}$), following similar notation of Tempelaar et al.⁵ When the samples are considered homogeneous throughout z, the matrices and resulting expressions become z-independent.⁵ The matrices f and F are segregated versions of the differential Mueller matrix (m), where the absorption (A) is removed such that the dichroic and birefringent effects can be considered alone, an attractive feature of Mueller matrix formalism; f corresponds to the matrix of per unit length effects; F corresponds to the matrix of total effects for a sample.5,7,35

The exponential form of the Mueller matrix $(M_z = e^{mz})$ is convenient because it can be approximated with a Taylor expansion, allowing one to solve Equation (2) using matrix multiplication alone: 35,45

$$M_{z(1)} = e^{mz} = e^{a\mathbb{1}z + F} = e^{a\mathbb{1}z}e^F = e^{a\mathbb{1}z}[\mathbb{1} + F + ...] \qquad (4)$$

$$M_{z(2)} = e^{mz} = e^{a\mathbb{1}z + F} = e^{a\mathbb{1}z}e^F = e^{a\mathbb{1}z}\left[\mathbb{1} + F + \frac{1}{2!}F^2 + \dots\right] \tag{5}$$

$$M_{z(3)} = e^{mz} = e^{a\mathbb{1}z + F} = e^{a\mathbb{1}z}e^{F} = e^{a\mathbb{1}z}\left[\mathbb{1} + F + \frac{1}{2!}F^{2} + \frac{1}{3!}F^{3} + \dots\right]$$
 (6)

where Equations (4)–(6) use expansions to the first-, second-, and third-order, respectively. Because the sample can be rotated azimuthally about the light propagation direction throughout the measurement, a rotation matrix is applied to M_z , which gives us the angular dependent Mueller matrices $M'(\theta)$ with the first-, second-, and third-order Taylor expansion expressions. These expressions are substituted into Equations (2) to compute the Stokes vector for the output light (S_{out}):

$$S_{out} = R(-\theta)M_zR(\theta)S_{in} = M'(\theta)S_{in}$$
 (7)

The first component of the S_{out} vector (I_{detect} , the total intensity of output light) is extracted to calculate the experimentally measured CD signal (I_{CD}). A lock-in amplifier processes the I_{detect} into AC and DC components, and the ratio between the AC and DC signals yields the measured CD signal (I_{CD}) (details in the Supporting Information).

The order to which the exponential e^F is expanded (Equations 4–6) makes a significant change to the expression for the measured CD (see the Supporting Information for full derivation details). If the exponential is expanded only to the first-order, I_{CD} only contains the chirality-induced CD (CDchiroptic) term caused by chiral structures and assemblies (differential absorption of leftand right-circularly polarized light caused by structural chirality), along with a term caused by residual static birefringence of the photoelastic modulator (CD_a) that is present in all expressions^{7,31} (Equation 8; Table S1). (Note: We choose the nomenclature CD_{chiroptic} over others such as "true" CD because it gives the impression that measured CD caused by LDLB is somehow "false" or "artifactual" although it is not since this signal can accurately be described as a difference in the absorbance between left-circularly polarized and right-circularly polarized light, or CD. Additionally, we find the term "chiroptic" to be informative: It denotes optical activity induced by chiral matter.) A second-order expansion is the most standard expression, which yields three terms in the expression for the measured CD: $I_{CD} = CD_{chiroptic} +$ $CD_{LDLB} + CD_{\alpha}$ (Equation 9; Table S1). Finally, if the exponential is expanded to the third-order, additional macroscopic anisotropy terms are introduced to the expression, coined "pairwise interference" terms by Jensen and Schellman et al.³⁵ (Equation 10; Table S1). These first three expansions can be written using their full expressions (Table S1) or with abbreviated names for each term (Equations 8-10):

$$I_{CD(1)} = CD_{chiroptic} + CD_{\alpha} \tag{8}$$

Order	Expressions for measured CD
(1)	$I_{CD} = G_0[CD] = CD_{chiroptic}$
(2)	$I_{CD} = G_0 \left[CD + \frac{1}{2} (LB \cdot LD' - LD \cdot LB') \right] = CD_{chiroptic} + CD_{LDLB}$
(3)	$I_{CD} = G_0 \left[CD + \frac{1}{2} (LB \cdot LD' - LD \cdot LB') + \frac{1}{6} \left(CD \left(CD^2 + LD^2 + LD'^2 \right) - LB (CD \cdot LB + CB \cdot LD) - LB' (CD \cdot LB' + CB \cdot LD') \right) \right]$
	$= CD_{chiroptic} + CD_{LDLB} + CD_{pairwise}$

$$I_{CD(2)} = CD_{chiroptic} + CD_{LDLB} + CD_{\alpha}$$
 (9)

$$I_{CD(3)} = CD_{chiroptic} + CD_{LDLB} + CD_{pairwise} + CD_{\alpha}$$
 (10)

Beyond this point, we will not include the artifacts introduced by the photoelastic modulator (PEM) (CD_{α}) because these effects can be removed by averaging over multiple azimuths,⁴⁰ although only two measurements separated by 90° are necessary.^{7,46} Throughout this work, we assume these terms have been removed through azimuthal averaging, a best practice for all chiroptical experimentalists (Table 1).

Recently discussed by Tempelaar et al.⁴ and demonstrated by Lu et al.,⁵ the relative contribution of each term to the CD spectrum is sample thickness-dependent: $CD_{chiroptic}$ has a linear scaling with (z), CD_{LDLB} has a square scaling (z^2) , and $CD_{pairwise}$ has a cubic scaling (z^3) . The full expressions are displayed in Table S2.

Using the simplified expressions for the measured CD, we now consider the effects of the higher-order terms on I_{CD} and the difference between these terms relative to the contributions of $CD_{chiroptic}$ using numerical simulations. For simplicity, we consider each of the optical phenomenon to be normalized, where LD, LD', and CD range from [-1,1] and LB, LB', and CB range from $[-\pi, \pi]$ (Supporting Information).

3 | RESULTS AND DISCUSSION

To demonstrate the impact of the different expansion approximations of the CD signal for an anisotropic sample, we use simple Lorentzian lineshape functions to represent each optical phenomenon (LD, LB, LD', LB', CD, and CB) (details in the Supporting Information) and plot the output signal for each of the approximations. As an example of errors induced by the second-order approximation, we consider a sample that has weak chiral anisotropy ($CD \sim 10^{-6}$) characteristic of small molecules but has strong linear anisotropy (LD, $LD' \sim 10^{-1}$), characteristic of oriented samples. We choose to set LB, $LB' \sim -10^{-2}$ and CB = 0, reasonable values for an oriented,

chiral sample (full details for each parameter in the Supporting Information). Inserting these values into the second-order expansion, we find that, due to the LDLB interactions, the measured CD signal (I_{CD}) on a commercial CD spectrometer would register a signal maximum that is three orders of magnitude stronger than the chirality-induced CD of the sample ($CD_{chiroptic}$) (Figure 1A, black plot vs. red plot). Including third-order terms from the pairwise interactions does not further distort or repair this error (Figure 1A, blue plot). The LDLB artifact can clearly present exceedingly erroneous CD signals for anisotropic samples.

In the case of a sample with strong linear and circular dichroism, the pairwise interference term influences the measured spectra, distorting the spectra beyond its intrinsic chiroptic CD signal. For example, when there is strong chiral anisotropy $(CD \sim 10^{-2})$ in addition to the linear anisotropy $(LD \sim 10^{-1})$, along with other reasonable parameters $(LB, LB' \sim -10^{-2}, LD' \sim 10^{-1})$, and $CB \sim 10^{-3}$, the second- and third-order contributions can nearly double I_{CD} (Figure 1B, black plot vs. blue plot). The pairwise interference artifacts present subtle yet significant changes to CD spectra for strongly linearly and circularly dichroic samples.

To examine the effect of the full parameter space of linear and chiral anisotropy on the measured signal and the calculated approximations, we vary the CD (CD_{chirontic}) and LD while holding other parameters constant and compute the first-, second-, and third-order approximations of the measured CD peak signal (I_{CD}) (Table 1 and Figure 2). We consider the case of a highly oriented and anisotropic sample with $CB = \pi \times CD$, LB = LD, LD' = 0.2, and LB' = 0. These sample values are carefully selected to represent state-of-the-art, highly oriented materials.¹⁴ In these plots, the x- and y-axes are the CD and LD terms, respectively, and the color gradient indicates the I_{CD} value, considering first-, second-, or third-order approximations of the signal $(CD_{chiroptic}, CD_{chiroptic} + CD_{LDLB}, \text{ and } CD_{chiroptic} + CD_{LDLB}$ $+CD_{pairwise}$, respectively). As a control, a contour plot of CD_{chiroptic} against changes in LD and CD results, as expected, in no influence of the CD and LD terms on the measured value: There is and should be a direct match

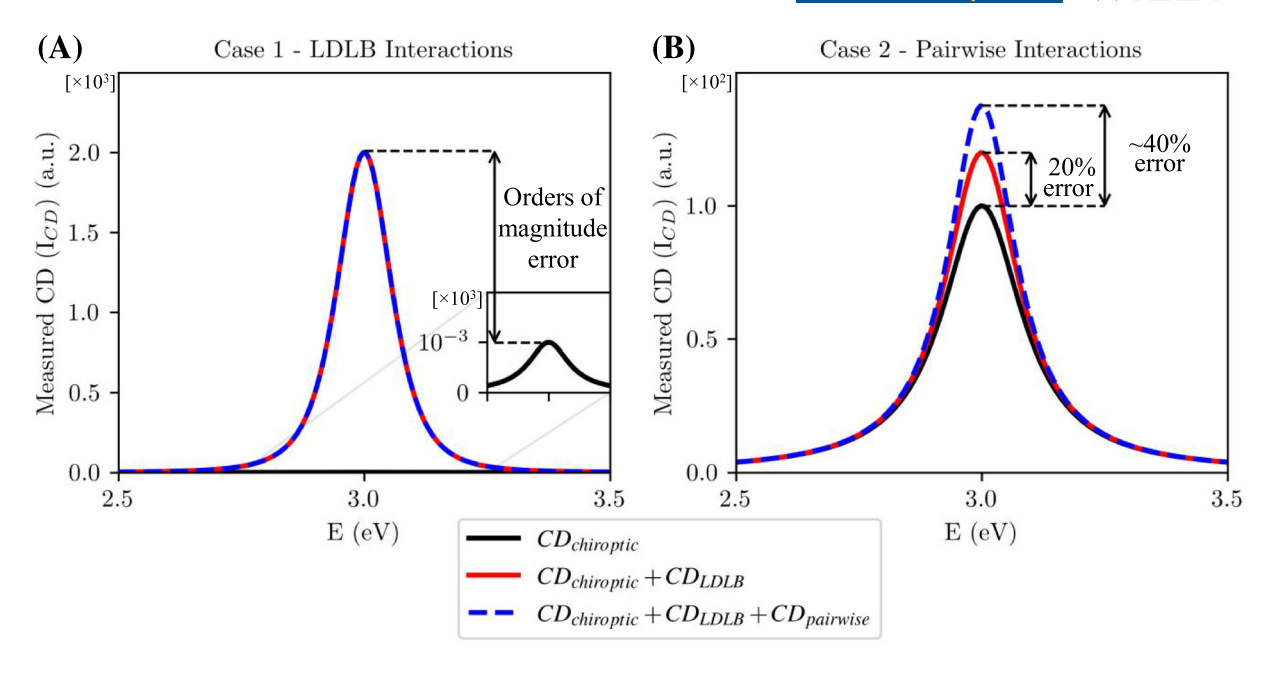


FIGURE 1 Errors between measured circular dichroism spectra and chirality-induced circular dichroism spectra for anisotropic samples. The measured CD is computed with increasing accuracy using simulated spectra for LD, LB, LD', LB', CD, and CB (simulated as Lorentzian functions, their Hilbert transforms, and Ricker functions [Figure S1]). The measured CD is first computed only from contributions of the chirality-induced, or chiroptic, CD (black plots), then with additions of the LDLB second-order term (red plots), and further with the addition of the third-order pairwise term (blue plots). (A) Simulated measured CD spectra for a representative sample with weak chirality but strong linear anisotropy [LD \sim 0.9, LD' \sim 0.43, LB, LB' \sim -10⁻², CD \sim 10⁻⁶, CB = 0]. Due to LDLB interactions, the measured CD, alarmingly, demonstrates a three orders of magnitude increase from the chiroptic CD. The inclusion of pairwise interactions caused by the higher-order expansion does not further distort this artifact signal. (B) Simulated measured CD spectra for a representative sample with strong chirality and strong linear anisotropy [LD \sim 0.9, LD' \sim 0.43, LB, LB' \sim -10⁻², CD \sim 10⁻², CB \sim 10⁻³]. The measured CD computed using a more accurate, third-order approximation (blue plot) demonstrates up to a 40% difference compared to the chiroptic CD (black plot). Simulated spectra used to represent the six optical phenomena (LD, LB, LD', LB', CD, and CB) can be found in Figure S1.

between the input CD (CD_{chiroptic}) and the measured CD (I_{CD}) because no interference effects are being considered (Figure 2A). When second-order effects are included $(I_{CD} = CD_{chiroptic} + CD_{LDLB})$, the contour intensities are no longer the same as the input, demonstrating the inclusion of LDLB interactions in the measured CD. Finally, a curvature appears in the plots when third-order effects are included as well $(I_{CD} = CD_{chiroptic} + CD_{LDLB} + CD_{pairwise}),$ indicating that the magnitude of the measured CD signal experiences a nonlinear divergence from CD_{chiroptic} due to interactions between a sample's dichroic and birefringent properties. To demonstrate the variability possible in measured spectra, other representative samples are considered in Figures S2-S4.

The inaccuracy in the measured signal from the chirality-induced CDcan be computed as the percent error between and I_{CD} $CD_{chiroptic}$ $\left(\%error = \frac{I_{CD} - CD_{chiroptic}}{CD_{chiroptic}} \times 100\right)$ (Figure 2D,E for the error in the second-order (D) and third-order (E) expansions). The largest error for the LDLB artifacts is about the y-axis, where the chiroptic CD is near 0 (Figure 2D); this high %error is caused by dividing a finite number by the

denominator approaching 0 in the expression. In the regions outside of this $CD \sim 0$ band, the error never exceeds more than 20%. The error exposed by the thirdorder approximation follows a more complicated relationship with the CD and LD. For a constant, positive CD value, the error increases as LD increases, going beyond 100% error as the CD approaches 0. And this behavior is mirrored inversely for constant, negative values of CD: The error increases as LD decreases beyond 100% error as CD approaches 0 (at which point the error is undefined). This convoluted behavior is because the pairwise equation introduces cubic terms, which blow up in the strongly linearly and circularly dichroic parameter space. Thus far, our analysis reveals that the measured CD signal can stray far from the chiroptical CD signal.

Although these errors introduced by the LDLB and pairwise terms are outrageously high, we have shown in our previous work that the LDLB error can be corrected for, reducing the overall measurement error. To remove LDLB interactions, the I_{CD} signal is collected and averaged over two scans before and after rotating the sample against the beam axis. The measured CD is then

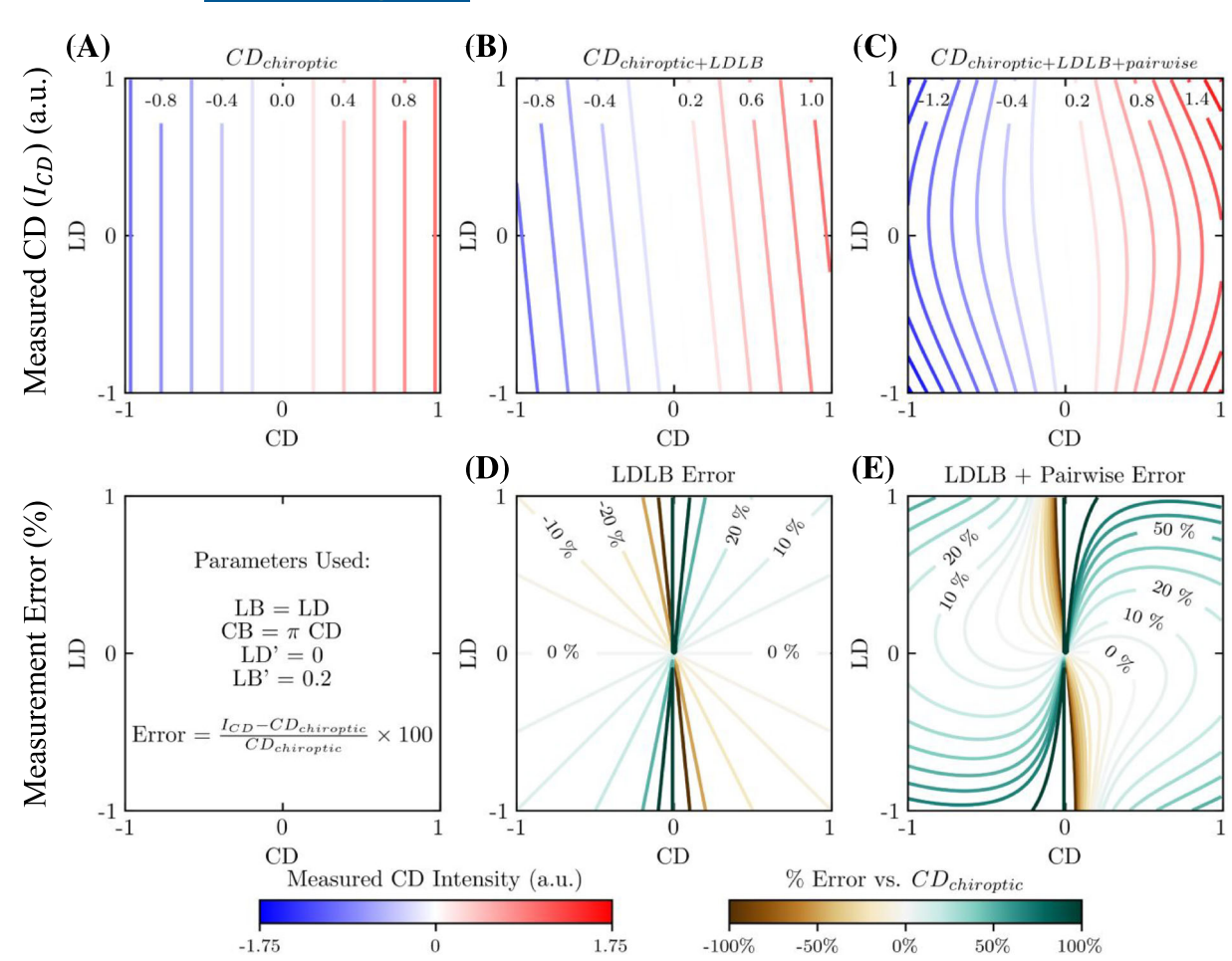


FIGURE 2 Measured CD intensity as a function of chirality-induced CD and LD for first-, second-, and third-order approximation expansion (top row) and corresponding error between the measured spectra and the chirality-induced CD spectra (bottom row) for anisotropic samples. (A–C) Contour plots of numerically simulated CD that would be measured by a commercial instrument as a function of chiroptic CD and LD considering only the first-order chiroptic CD term (A), both the first- and second-order (LDLB interactions) terms (B), and the first-, second-, and third-order (pairwise interactions) terms (C). The *x*-axis is the sample's input chiroptic CD parameter, the *y*-axis the sample's input LD, and the blue-white-red color gradient is the resulting measured CD intensity. Note: every point on these plots corresponds to a different sample. (D,E) Plots of error in CD between the measured CD and the chiroptic CD, for the case of second-order approximation expansion including LDLB interactions (D) and for the case of the third-order approximation expansion including both LDLB and pairwise interactions (E). Due to the definition of error, the percent error approaches infinity as the chiroptic CD approaches 0 (a divide by 0 error).

just a combination of the chirality-induced CD and the pairwise artifact ($I_{CD} = CD_{chiroptic} + CD_{pairwise}$) (Figure 3). The remaining error between the $CD_{chiroptic} + CD_{pairwise}$ and the $CD_{chiroptic}$ is less severe compared with when the LDLB contributions are included (compare Figure 2C to Figure 3A), but the values are still substantially large for highly anisotropic samples. In regions of high linear and circular dichroism, there are large spurious contributions from these pairwise interference terms. For example, considering a material with LD = 0.8 and CD = 0.8 (which corresponds to g-factor = 1.6), the measured CD considering the pairwise term ($CD_{corrected} = CD_{chiroptic} + CD_{pairwise}$) would be 1.16 units, a 45% error from the $CD_{chiroptic}$ value, 0.8 units.

These significant errors highlight an alarming issue concerning these third-order, pairwise interference contributions: the inability to remove their presence from the spectra. Typically, antisymmetric LDLB interactions can be removed, considered, and interpreted by measuring samples through their front and back faces. The pairwise interference terms, however, cannot be removed and they may cause an artificial increase or decrease in the measured CD of strongly linearly and circularly dichroic materials (see the Supporting Information). In light of the persistent influence of higher-order pairwise interactions on the measurement of CD, which impacts the magnitude (and lineshape) (Figures S3 and S4) of the CD spectra compared to the chiroptic CD, our objective

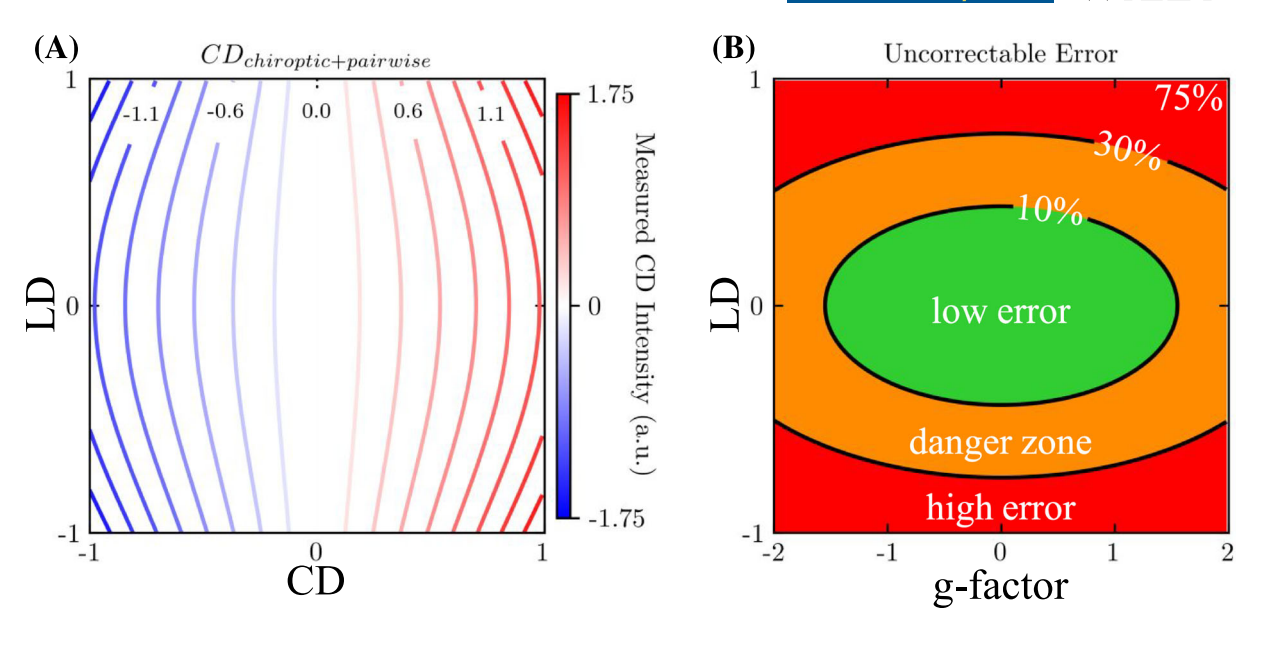


FIGURE 3 Measured CD intensity as a function of chirality-induced CD and LD for the corrected measured CD and the error between them. (A) Measured CD intensity as a function of chiroptic CD and LD considering terms up to the third-order approximation but correcting for the second-order LDLB interactions. (B) The percent error between chiroptic CD (Figure 2A) and corrected CD (A), plotted in terms of the dissymmetry factor (g-factor $\equiv 2\frac{A_R-A_L}{A_R+A_L} = \frac{CD}{A}$, where A_R , A_L are the absorption of right- and left-circularly polarized light, respectively.) (B), demarcated into regions in which errors are reasonable or not reasonable. Regions colored green indicate a <10% error, regions colored orange indicate an error between 10% and 30%, and regions in red indicate a >30% error between the measured peak value and the chiroptic CD value. To represent highly oriented and anisotropic samples, we choose to set CB equal to CD × π , LB = LD, and LB' = LD' = 0. ¹³

is to encourage readers to consider the material systems that may be affected by this phenomenon. To present this information in a more accessible form, we will show how this uncorrectable error also distorts the g-factor (dissymmetry factor, ²⁹ g-factor $\equiv 2\frac{A_R - A_L}{A_R + A_L} = \frac{CD}{A}$) (Figure 3B). For example, the biomimetic photonic films produced by Tang et al., 23,27 which demonstrate a g-factor between 1 and 1.6 and LD > 0.2 would present errors at least greater than 15% based on our assessment. By plotting the g-factor along the x-axis instead of the CD, one can identify the regions in the parameter space where significant errors are likely to occur. This serves as a useful reference for determining potentially problematic areas. Regions with low error (<10%) are colored in green. Measurements from samples that fall in this space are safe to trust. The parameter space that produces errors between 10% and 30% is colored in orange. Measurements of samples that fall in this moderately anisotropic region should be taken with caution. Finally, linearly anisotropic and circularly dichroic regions that produce >30% difference are colored in red. Measurements from samples that land in this region should not be trusted; instead, the experimentalist should collect spectra from these samples using Mueller matrix polarimeters (MMPs), which yield spectra for the entire Mueller matrix, uncompromised by higherorder effects.44

We note that this is also the case for samples that are thick and strongly depolarizing: These samples too should be measured on an MMP. In general, depolarization is a phenomenon to be wary of when measuring circular dichroism with a CD spectrometer. Imagining a circular dichroism measurement as a one-shot interaction is not an accurate picture for most media: There are linear and circular diattenuation and retardation effects as well as depolarization effects. In the absence of incoherent scattering phenomena, the polarization state of light remains preserved along the entire path length solely within optically active media that is homogeneous. Conversely, in the case of inhomogeneous media, the initially circularly polarized incident light beam undergoes alterations in its polarization state along the path length due to the complex effects arising from the media's nonuniformity. Unfortunately, depolarization cannot be easily measured without a polarimetric technique (e.g., MMP), but experimenters can develop a feel for a sample's depolarization by measuring CD of samples at varying thicknesses. 44,49,50 Because CD follows Beer's law, CD scales linearly with pathlength or film thickness. 36,51,52 Significant deviations from this linear curve should raise concerns of significant depolarization effects; the depolarization origins can vary in inhomogeneous media. 49,53 The CD properties of significantly depolarizing samples

1520636x, 0, Downloaded from https://onlinelibrary.wiley.com/doi/10.1002/chir.23597 by Cornell University, Wiley Online Library on [1807/2023]. See the Terms and Conditions (https://onlinelibrary.wiley.com/terms-and-conditions) on Wiley Online Library for rules of use; OA articles are governed by the applicable Creative Commons License and Conditions (https://onlinelibrary.wiley.com/terms-and-conditions) on Wiley Online Library for rules of use; OA articles are governed by the applicable Creative Commons License and Conditions (https://onlinelibrary.wiley.com/terms-and-conditions) on Wiley Online Library for rules of use; OA articles are governed by the applicable Creative Commons License and Conditions (https://onlinelibrary.wiley.com/terms-and-conditions) on Wiley Online Library for rules of use; OA articles are governed by the applicable Creative Commons License and Conditions (https://onlinelibrary.wiley.com/terms-and-conditions) on Wiley Online Library for rules of use; OA articles are governed by the applicable Creative Commons License and Conditions (https://onlinelibrary.wiley.com/terms-and-conditions) on Wiley Online Library for rules of use; OA articles are governed by the applicable Creative Commons License and Conditions (https://onlinelibrary.wiley.com/terms-and-conditions) on Wiley Online Library for rules of use; OA articles are governed by the applicable Creative Commons and Conditions (https://onlinelibrary.wiley.com/terms-and-conditions) of the applicable Creative Commons and Co

are unable to be measured through typical benchtop instruments and must be studied with an MMP.

We note also that in a recent theoretical study by Gao has revealed that even in deterministic media, the interference between dichroism and birefringence leads to the loss of the symmetry properties of the Mueller matrix in anisotropic systems. 54,55 The loss of the symmetry in the Mueller matrix prohibits certain uses of the differential Mueller matrix and increases the difficulty of interpreting the Mueller matrices and circular dichroism spectra of anisotropic media.

4 | CONCLUSION

In summary, we have derived a more accurate expression for the measured CD using a third-order Taylor series expansion on the exponential form of the Mueller matrix. rather than the standard second-order expansion. This more accurate expansion introduces a new term to the expression for measured CD, coined the "pairwise interference" term. Unlike the LDLB interference term, we find that the pairwise interference term cannot be averaged out from measured spectra even with clever averaging schemes. Using numerical simulations, we first show that the LDLB interference can manifest as CD signals three orders of magnitude stronger than the chiral anisotropy characteristic of the sample, reaffirming the growing literature precedent of the importance of LDLB interaction. Then, we demonstrate that the pairwise interference terms lead to spurious contributions to the measured CD spectra for samples with moderate-to-high anisotropy, capable of changing CD peak intensities by a factor of more than two and altering spectra lineshapes, in particular for thick samples (Figures S3-S5). These complex effects are due to the cubic, pairwise interference between the six dichroic and birefringent properties (LD, LB, LD', LB', CD, and CB) in ordered samples. By computing the percent error between the more accurate, third-order expression derived in this work and the chirality-induced CD over a wide parameter space, we leave readers with guidance for studying the circular dichroism in anisotropic media; media with little linear anisotropy are free from these pairwise interference effects, whereas media with moderate-to-strong linear anisotropy are at extreme danger of being affected. By extension, these moderately to strongly anisotropic samples are at risk of fourth- and higher-order contributions, although not explicitly evaluated in this work. Measurements of state-of-the-art, strongly linearly and circularly dichroic samples will be impacted by these effects in a manner that is significant yet difficult to detect without measurement of the entire Mueller matrix. The derived

expression and numerical simulations presented in this work emphasize the importance of revisiting the growing literary precedent for LDLB interactions, as well as the awareness of higher-order pairwise interference effects in highly ordered media.

5 | DERIVATION NOTE

In our previous work, 7 we used uppercase letters (LD, LB, LD', LB', CD, and CB) in the Mueller matrix to represent the per unit length notation. This notation yields expressions including a thickness scaling, a factor of z in front of $CD_{chiroptic}$ and a factor of z^2 in front of CD_{LDLB} (discussed in derivation; Table S2). In this work, we choose to use the notation of Tempelaar et al., 5 where lowercase letters (ld, lb, ld', lb', cd, and cb) correspond to the per unit length notation. The uppercase letters instead correspond to the total dichroic and birefringent effects of the sample being considered.

This notation follows through into the notation for our segregated differential Mueller matrices $(f = \frac{F}{z})$. The matrix F in our previous work corresponds to the matrix f in this work.

The expressions (1), (2), and (3) correspond to the derived expressions using first-, second-, and third-order Taylor expansions (see Equations (4)–(6) and (8)–(10)). As the expansion is taken to higher-orders (and thus, higher accuracies), additional terms are introduced with spurious contributions to the measured CD. The chiroptic term corresponds to the chirality-induced CD, the firstorder term Taylor expansion of e^{mz} (Equation 6). The LDLB term corresponds to the LDLB interaction term, caused by the misalignment of the LD and LB principal axes, the second-order term in the Taylor expansion of e^{mz} (Equation 8). The pairwise term corresponds to the new term derived in this work, the third-order term in the Taylor expansion of e^{mz} (Equation 9). The G_0 term is a constant determined by the operating parameters of the circular dichroism spectrometer $(G_0 = \frac{1}{2}J_1(A)\cos$ $\left(\varphi_{signal} - \varphi_{lock-in}\right) \nu_{lock-in}$, where $J_1(A)$ denotes a Bessel function of the first-order and was introduced during lock-in processing (from the expansion of sine and cosine functions), $\nu_{lock-in}$ is the operating frequency of the lockin amplifier, A is the general amplitude, and φ is the general phase. 7,35,56 Throughout this work, we set $G_0 = 1$ for simplicity.

ACKNOWLEDGMENTS

This work was supported in part by the National Science Foundation (NSF) under Award Nos. DMR-2003431 and CHE-2003586. This work made use of the Cornell Center for Materials Research Shared Facilities, which are supported through the NSF MRSEC program (DMR-1719875). We would like to thank Professor David J. Norris for the helpful suggestions.

DATA AVAILABILITY STATEMENT

The data that supports this work are available from the corresponding author upon reasonable request.

ORCID

Thomas J. Ugras https://orcid.org/0000-0002-5931-3031 *Yuan Yao* https://orcid.org/0000-0002-4784-2753 Richard D. Robinson https://orcid.org/0000-0002-0385-2925

REFERENCES

- 1. Shindo Y, Nishio M. The effect of linear anisotropies on the CD spectrum: is it true that the oriented polyvinyalcohol film has a magic chiral domain inducing optical activity in achiral mole-Biopolymers. 1990;30(1-2):25-31. doi:10.1002/bip. 360300105
- 2. Kuroda R, Harada T, Shindo Y. A solid-state dedicated circular dichroism spectrophotometer: development and application. Rev Sci Instrum. 2001;72(10):3802-3810. doi:10.1063/1.1400157
- 3. Albano G, Lissia M, Pescitelli G, Aronica LA, Di Bari L. Chiroptical response inversion upon sample flipping in thin films of a chiral benzo[1,2-b:4,5-B']dithiophene-based oligothiophene. Mater Chem Front. 2017;1(10):2047-2056. C7QM00233E
- 4. Albano G, Górecki M, Jávorfi T, et al. Spatially resolved chiroptical study of thin films of benzo[1,2-b:4,5-b']dithiophene-based oligothiophenes by synchrotron radiation electronic circular dichroism imaging (SR-ECDi) technique. Aggregate. 2022;3(5): e193. doi:10.1002/agt2.193
- 5. Salij A, Goldsmith RH, Tempelaar R. Theory of apparent circular dichroism reveals the origin of inverted and noninverted chiroptical response under sample flipping. J Am Chem Soc. 2021;143(51):21519-21531. doi:10.1021/jacs.1c06752
- 6. Zhang Z, Wang Z, Sung HH-Y, Williams ID, Yu Z-G, Lu H. Revealing the intrinsic chiroptical activity in chiral metalhalide semiconductors. J Am Chem Soc. 2022;144(48):22242-22250. doi:10.1021/jacs.2c10309
- 7. Yao Y, Ugras TJ, Meyer T, et al. Extracting pure circular dichroism from hierarchically structured CdS magic cluster films. ACS Nano. 2022;16(12):20457-20469. doi:10.1021/ acsnano.2c06730
- Wade J, Salerno F, Kilbride RC, et al. Controlling anisotropic properties by manipulating the orientation of chiral small molecules. Nat Chem. 2022;14(12):1383-1389. doi:10.1038/s41557-022-01044-6
- 9. Freudenthal JH, Hollis E, Kahr B. Imaging chiroptical artifacts. Chirality. 2009;21(1E):E20-E27. doi:10.1002/chir.20768
- 10. Zhou S, Li J, Lu J, et al. Chiral assemblies of pinwheel superlattices on substrates. Nature. 2022;612(7939):259-265. doi:10. 1038/s41586-022-05384-8
- 11. Lightner CR, Desmet F, Gisler D, et al. Understanding artifacts in chiroptical spectroscopy. ACS Photonics. 2023;10(2):475-483. doi:10.1021/acsphotonics.2c01586

- 12. Disch RL, Sverdlik DI. Apparent circular dichroism of oriented systems. Anal doi:10.1021/ ac60270a038
- 13. Davidsson Å, Nordén B, Seth S. Measurement of oriented circular dichroism. Chem Phys Lett. 1980;70(2):313-316. doi:10. 1016/0009-2614(80)85341-3
- 14. Schellman J, Jensen HP. Optical spectroscopy of oriented mole-Chem Rev. 1987;87(6):1359-1399. cr00082a004
- 15. Shindo Y, Ohmi Y. Problems of CD spectrometers. 3. Critical comments on liquid crystal induced circular dichroism. J Am Chem Soc. 1985;107(1):91-97. doi:10.1021/ja00287a017
- 16. Shindo Y. Application of polarized modulation technique in polymer science. Optim Eng. 1995;34(12):3369-3384. doi:10. 1117/12.213252
- 17. Tinoco I Jr, Cantor CR. Application of optical rotatory dispersion and circular dichroism to the study of biopolymers. In: Methods of Biochemical Analysis. John Wiley & Sons, Ltd; 1970: 81-203. doi:10.1002/9780470110362.ch3
- 18. Go N. Optical activity of anisotropic solutions. I J Chem Phys. 1965;43(4):1275-1280. doi:10.1063/1.1696914
- 19. Go N. Optical activity of anisotropic solutions. II. J Phys Soc Jpn. 1967;23(1):88-97. doi:10.1143/JPSJ.23.88
- 20. Kuball H-G, Karstens T. Optical activity of oriented molecules. Angew Chem Int Ed Engl. 1975;14(3):176-177. doi:10.1002/anie. 197501761
- 21. Disch RL, Sverdlik DI. Anisotropy of molecular optical rotation. I transparent media. J Chem Phys. 1967;47(6):2137-2148. doi:10.1063/1.1712247
- 22. Hirschmann M, Merten C, Thiele CM. Treating anisotropic artefacts in circular dichroism spectroscopy enables investigation of lyotropic liquid crystalline polyaspartate solutions. Soft Matter. 2021;17(10):2849-2856. doi:10.1039/D0SM02102D
- 23. Lv J, Ding D, Yang X, et al. Biomimetic chiral photonic crystals. Angew Chem Int Ed. 2019;58(23):7783-7787. doi:10.1002/ anie.201903264
- 24. Chen L, Hao C, Cai J, et al. Chiral self-assembled film from semiconductor nanorods with ultra-strong circularly polarized luminescence. Angew Chem Int Ed. 2021;60(50):26276-26280. doi:10.1002/anie.202112582
- 25. Yeom B, Zhang H, Zhang H, et al. Chiral plasmonic nanostructures on achiral nanopillars. Nano Lett. 2013;13(11):5277-5283. doi:10.1021/nl402782d
- 26. Wilson JN, Steffen W, McKenzie TG, et al. Chiroptical properties of poly(p-phenyleneethynylene) copolymers in thin films: large g-values. J Am Chem Soc. 2002;124(24):6830-6831. doi:10. 1021/ja026532s
- 27. Lv J, Hou K, Ding D, et al. Gold nanowire chiral ultrathin films with ultrastrong and broadband optical activity. Angew Chem Int Ed. 2017;56(18):5055-5060. doi:10.1002/anie.201701512
- 28. Albano G, Salerno F, Portus L, Porzio W, Aronica LA, Di Bari L. Outstanding chiroptical features of thin films of chiral oligothiophenes. ChemNanoMat. 2018;4(10):1059-1070. doi:10. 1002/cnma.201800244
- 29. Albano G, Pescitelli G, Di Bari L. Chiroptical properties in thin films of π -conjugated systems. Chem Rev. 2020;120(18):10145-10243. doi:10.1021/acs.chemrev.0c00195
- 30. Salij AH, Goldsmith RH, Tempelaar R. Chiral polaritons based on achiral Fabry-Perot cavities using apparent circular

- dichroism. arXiv 27, 2022. http://arxiv.org/abs/2208.14461 (accessed 2023-02-03).
- 31. Arteaga O, Kahr B. Mueller matrix polarimetry of bianisotropic materials [invited]. *J Opt Soc Am B.* 2019;36(8):F72. doi:10. 1364/JOSAB.36.000F72
- 32. Arteaga O, Maoz BM, Nichols S, Markovich G, Kahr B. Complete polarimetry on the asymmetric transmission through subwavelength hole arrays. *Opt Express.* 2014;22(11):13719-13732. doi:10.1364/OE.22.013719
- 33. Martin AT, Nichols SM, Murphy VL, Kahr B. Chiroptical anisotropy of crystals and molecules. *Chem Commun*. 2021; 57(66):8107-8120. doi:10.1039/D1CC00991E
- 34. Han H, Kallakuri S, Yao Y, et al. Multiscale hierarchical structures from a nanocluster mesophase. *Nat Mater.* 2022;21(5): 518-525. doi:10.1038/s41563-022-01223-3
- Jensen HP, Schellman JA, Troxell T. Modulation techniques in polarization spectroscopy. *Appl Spectrosc.* 1978;32(2):192-200. doi:10.1366/000370278774331567
- Wan L, Wade J, Salerno F, et al. Inverting the handedness of circularly polarized luminescence from light-emitting polymers using film thickness. ACS Nano. 2019;13(7):8099-8105. doi:10. 1021/acsnano.9b02940
- Leite TR, Zschiedrich L, Kizilkaya O, McPeak KM. Resonant plasmonic-biomolecular chiral interactions in the far-ultraviolet: enantiomeric discrimination of Sub-10 nm amino acid films. *Nano Lett.* 2022;22(18):7343-7350. doi:10.1021/acs. nanolett.2c01724
- 38. Liu P, Chen W, Okazaki Y, et al. Optically active perovskite CsPbBr ₃ nanocrystals helically arranged on inorganic silica nanohelices. *Nano Lett.* 2020;20(12):8453-8460. doi:10.1021/acs. nanolett.0c02013
- Liu P, Battie Y, Decossas M, et al. Chirality induction to CdSe nanocrystals self-organized on silica nanohelices: tuning chiroptical properties. ACS Nano. 2021;15(10):16411-16421. doi:10. 1021/acsnano.1c05819
- 40. Ashoka A, Nagane S, Strkalj N, et al. Local symmetry breaking drives picosecond spin domain formation in polycrystalline semiconducting films.
- 41. Perrin F. Polarization of light scattered by isotropic opalescent media. *J Chem Phys.* 1942;10(7):415-427. doi:10.1063/1.1723743
- 42. Collett E. Field Guide to Polarization. SPIE; 2005. doi:10.1117/3. 626141
- 43. Hilfiker JN, Hong N, Schoeche S. Mueller matrix spectroscopic ellipsometry. *Adv Opt Technol.* 2022;11(3–4):59-91. doi:10.1515/aot-2022-0008
- Arteaga, O. Mueller matrix polarimetry of anisotropic chiral media, 2010.
- 45. Troxell TC, Scheraga HA. Electric dichroism and polymer conformation. I. Theory of optical properties of anisotropic media, and method of measurement. *Macromolecules*. 1971;4(5):519-527. doi:10.1021/ma60023a001
- 46. Tunis-Schneider MJ, Maestre MF. Circular dichroism spectra of oriented and unoriented deoxyribonucleic acid films--a

- preliminary study. *J Mol Biol.* 1970;52(3):521-541. doi:10.1016/0022-2836(70)90417-1
- 47. Pham T-T-H, Lo Y-L. Extraction of effective parameters of anisotropic optical materials using a decoupled analytical method. *J Biomed Opt.* 2012;17(2):025006. doi:10.1117/1.JBO. 17.2.025006
- 48. Lu S-Y, Chipman RA. Interpretation of Mueller matrices based on polar decomposition. *JOSA A*. 1996;13(5):1106-1113. doi:10. 1364/JOSAA.13.001106
- 49. Tompkins HG, Irene EA (Eds). *Handbook of Ellipsometry*. William Andrew Pub.; Springer; 2005.
- Krishnan S, Nordine PC. Mueller-matrix ellipsometry using the division-of-amplitude photopolarimeter: a study of depolarization effects. *Appl Optics*. 1994;33(19):4184-4192. doi:10.1364/ AO.33.004184
- 51. Schulz M, Zablocki J, Abdullaeva OS, et al. Giant intrinsic circular dichroism of prolinol-derived squaraine thin films. *Nat Commun*. 2018;9(1):2413. doi:10.1038/s41467-018-04811-7
- 52. Tang Q, Zhao L, Xie J, Liu K, Liu W, Zhou S. Deviations from Beer's law in electronic absorption and circular dichroism: detection for enantiomeric excess analysis. *Chirality*. 2019; 31(7):492-501. doi:10.1002/chir.23072
- Craig MR, Jonkheijm P, Meskers SCJ, Schenning APHJ, Meijer EW. The chiroptical properties of a thermally annealed film of chiral substituted polyfluorene depend on film thickness. *Adv Mater*. 2003;15(17):1435-1438. doi:10.1002/adma. 200305243
- 54. Gao W. Coupling effects between dichroism and birefringence of anisotropic media. *Phys Lett A*. 2020;384(27):126699. doi:10. 1016/j.physleta.2020.126699
- 55. Gao W. Coupling effects among elementary polarization properties. *Sci Rep.* 2021;11(1):1328. doi:10.1038/s41598-020-79174-5
- Arteaga O, Freudenthal J, Wang B, Kahr B. Mueller matrix polarimetry with four photoelastic modulators: theory and calibration. *Appl Optics*. 2012;51(28):6805-6817. doi:10.1364/AO. 51.006805

SUPPORTING INFORMATION

Additional supporting information can be found online in the Supporting Information section at the end of this article.

How to cite this article: Ugras TJ, Yao Y, Robinson RD. Can we still measure circular dichroism with circular dichroism spectrometers: The dangers of anisotropic artifacts. *Chirality*. 2023; 1-10. doi:10.1002/chir.23597